TITLE:
Manufacture and drug delivery applications of silk nanoparticles

AUTHORS:
Wongpinyochit, Thidarat
Strathclyde Institute of Pharmacy and Biomedical Sciences
University of Strathclyde
Glasgow, Scotland, UK
thidarat.wongpinyochit@strath.ac.uk

Johnston, Blair F.
Strathclyde Institute of Pharmacy and Biomedical Sciences
University of Strathclyde
Glasgow, Scotland, UK
Blair.Johnston@strath.ac.uk

Seib, F. Philipp
Strathclyde Institute of Pharmacy and Biomedical Sciences
University of Strathclyde
Glasgow, Scotland, UK
Philipp.Seib@strath.ac.uk
Philipp.Seib@seiblab.com

CORRESPONDING AUTHOR:
F. Philipp Seib

SHORT ABSTRACT:
Nanoparticles are emerging as promising drug delivery systems for a broad range of indications. Here, we describe a simple yet powerful method to manufacture silk nanoparticles using reverse engineered *Bombyx mori* silk. These silk nanoparticles can be readily loaded with a therapeutic payload and subsequently explored for drug delivery applications.

LONG ABSTRACT:
Silk is a promising biopolymer for biomedical and pharmaceutical applications due to its outstanding mechanical properties, biocompatibility and biodegradability, as well its ability to protect and subsequently release its payload in response to a trigger. While silk can be formulated into various material formats, silk nanoparticles are emerging as promising drug delivery systems. Therefore, this article covers the procedures for reverse engineering silk cocoons to yield a regenerated silk solution that can be used to generate stable silk nanoparticles. These nanoparticles are subsequently characterized, drug loaded and explored as a potential anticancer drug delivery system. Briefly, silk cocoons are reverse engineered first by degumming the cocoons, followed by silk dissolution and clean up, to yield an aqueous silk solution. Next,

the regenerated silk solution is subjected to nanoprecipitation to yield silk nanoparticles – a simple but powerful method that generates uniform nanoparticles. The silk nanoparticles are characterized according to their size, zeta potential, morphology and stability in aqueous media, as well as their ability to entrap a chemotherapeutic payload and kill human breast cancer cells. Overall, the described methodology yields uniform silk nanoparticles that can be readily explored for a myriad of applications, including their use as a potential nanomedicine.

INTRODUCTION:
Nano-sized drug delivery systems are often used to control drug release and to deliver a diverse set of therapeutic payloads – for example, proteins, peptides and small molecular weight drugs – to target cells and tissues. These therapeutic payloads are often incorporated into various macromolecular drug carriers, such as liposomes, water soluble polymers (including dendrimers), and micro- and nanoparticles[1]. Nanoparticles (typically in a size range of 1 nm to 1,000 nm) are being widely explored as potential drug carriers, particularly for anticancer drug delivery[2]. The successful introduction of Abraxane (120 nm sized albumin-based nanoparticles loaded with paclitaxel) into routine clinical practice[3] has catalyzed the field, so that many more nanoparticles for drug delivery are now entering clinical trials[4]. Solid tumors generally show poor lymphatic drainage and have leaky blood vessels which means that nanoparticles of up to 200 nm will be passively targeted to these tumors following intravenous administration. This passive targeting phenomenon is called the enhanced permeability and retention (EPR) effect and was first reported in 1986[5]. The EPR effect can lead to a 50 to 100 fold increase in drug concentrations within the tumor microenvironment for a given drug dose when the drug payload is delivered using a macromolecular drug carrier approach rather than the free drug without the carrier. Drug-loaded nanoparticles designed for anticancer drug delivery have to reach the tumor microenvironment and often must enter a specific intracellular compartment, usually by endocytic uptake, for the drug to achieve its desired therapeutic effect[3]. Nanoparticles designed for intracellular drug delivery exploit endocytosis as a gateway into the cell as well as a route to overcome drug resistance mechanisms. Drug release from nanoparticles is often specifically designed to occur in lysosomes (i.e. lysosomotropic drug delivery)[6] where the pH responsiveness of the nanoparticle carrier (lysosomal pH approximately 4.5) can serve as trigger for drug release or lysosomal enzymes that liberate the payload from the carrier[7].

Many different classes of materials can be used to generate nanoparticles (e.g. metals and many organic and inorganic materials). However, biopolymers are emerging as attractive materials because of their known biocompatibility, biodegradability and low toxicity[8]. Many biopolymers are being explored, including albumin, alginate, chitosan and silk. Of these, silk has emerged as a promising contender for development into drug delivery systems[9]. Silks of various types are produced by a number of arthropods, including spiders (e.g. *Nephila clavipes*) and silkworms (e.g. *Bombyx mori*). Silkworm silk is used far more extensively than spider silk because the silkworm is fully domesticated and its silk thus represents a reproducible starting material. Silkworm silk is a Food and Drug Administration (FDA) approved material for human use, particularly as a suture material; it has a robust safety record in humans and is known to degrade *in vivo*[10]. The degradation profile of silk can be fine-tuned to range from hours (low crystalline silk) to 12 months or more (high crystalline silk). Silk degradation products are non-toxic and are metabolized in the body[10]. The silk structure imparts the ability to bind small molecular weight compounds and macromolecular protein drugs[11], making it a good material for controlled drug

release. Protein drugs (e.g. antibodies) are susceptible to denaturation, aggregation, proteolytic cleavage and clearance by the immune system. However, silk stabilizes therapeutic proteins due to the buffering capacity of its nanocrystalline regions and its ability to tailor water content at the nanoscale[11]. These unique features provide physical protection and reduce payload mobility[11] and are typically not seen with other (bio)polymers. Many anticancer drug delivery systems, for example silk-based hydrogels[12], films[13-15] and nanoparticles[16,17], have now been developed to exploit these features (reviewed in [18,19])

Here, silk nanoparticles were characterized by determining their size and charge over an extended time frame. Doxorubicin, a clinically relevant anticancer drug, was used as a model drug for drug loading and cytotoxicity studies in triple negative human breast cancer cells treated with drug-loaded silk nanoparticles.

PROTOCOL:

1.   Preparation of a reverse-engineered silk solution from *Bombyx mori* cocoons

Note: This methodology is based on protocols described elsewhere [12,27].

1.1)   Cut 5 g of dried cocoons with scissors into 5 mm × 5 mm pieces. Remove any soiled layers.

1.2)   Weigh out 4.24 g of sodium carbonate and add this carefully to 2 L of boiling distilled water.

Note: This yields a 0.02 M sodium carbonate solution.

1.3)   Add the cut cocoon pieces to the boiling sodium carbonate solution and boil for 60 minutes to degum the silk fibers. Stir the silk occasionally to ensure homogenous sample processing.

1.4)   Remove the degummed silk and wash with 1 L of distilled water for 20 minutes; repeat the washing step at least 3 times.

1.5)   Remove the washed silk and squeeze it well to remove excess liquid and then untie/pull the silk by hand. Place the untied silk in a fume hood to air dry overnight. This typically yields 3.6 g of degummed silk fibers.

1.6)   The next day, weigh out 5 g air-dried degummed silk fibers and pack the silk tightly into the bottom of a 50 mL beaker.

1.7)   Prepare a fresh 9.3 M LiBr solution. Dissolve the silk fibers in LiBr using a 1 g silk to 4 mL LiBr ratio. Cover the silk LiBr sample with aluminum foil to prevent evaporation and allow the silk to dissolve completely at 60°C. This step takes up to 4 hours and is aided by occasionally stirring.

1.8)   Wet a dialysis cassette (molecular weight cut-off of 3,500 Da) in water for 5 minutes. Inject 15 mL the silk LiBr solution into the 15 mL dialysis cassette and use a needle and syringe to remove any air bubbles.

1.9)   Dialyze against 1 L of distilled water and change the water at 1, 3 and 6 hours (i.e. 3 changes on the first day) and again on the next morning and evening (i.e. 2 changes on the second day), and again on the following morning (i.e. 1 change on the third day).

1.10)   Collect the silk solution from the dialysis cassette and centrifuge the solution for 20 minutes at 5 °C at 9500 x g. Recover the supernatant and repeat this centrifugation process twice more.

1.11)   Determine the weight of an empty weighing boat (W1) and add 1 mL of the silk solution. Record the weight again (W2) and then dry the sample by leaving the weighing boat at 60 ºC overnight. Next, determine the total dry weight (W3) (dried silk and weighing boat). The concentration of the silk solution (w/v) is: $\% = (W3-W1/W2-W1) \times 100$.

2.   Preparation of silk nanoparticles from reverse-engineered silk solution

2.1)   Add a 5% (w/v) silk solution dropwise to acetone while maintaining a >75% (v/v) acetone solution. For example, add 9 mL of a 5% (w/v) silk solution dropwise (10 μl/drop at a rate of 50 drops/minute) to 34 mL acetone.

2.2)   Centrifuge the precipitate at 48,000 x g for 2 hours at 4 °C.

2.3)   Aspirate the supernatant and resuspend the pellet in distilled water by first dislodging the pellet with a spatula and then adding 20 mL distilled water. Use pipet tips to remove the pellet from the spatula. After vortexing for 20 seconds followed by two sonication cycles using an ultrasonic probe at 30% amplitude for 30 seconds, top up the centrifuge tube to capacity with distilled water.

2.4)   Repeat the centrifugation and resuspension step at least twice.

2.5)   Resuspend the pellet in 6 mL distilled water, as detailed in 2.3 and store at 4 °C until use. For cell culture studies, silk nanoparticle stocks can be gamma irradiated [17].

3.   Determination of silk nanoparticle concentration

3.1)   Centrifuge silk nanoparticles at 48,000 x g for 2 hours at 4 °C.

3.2)   Collect all nanoparticles in 3 mL of distilled water, followed by two sonication cycles at 30% amplitude for 30 seconds.

3.3)   Divide the 3 mL stock of silk nanoparticles into 2 mL and 1 mL lots and transfer into pre-weighed 2 mL tubes. Record the total weight of the 2 mL sample. Store the 1 mL lot at 4 °C until use; this 1 mL sample will be used to generate a calibration curve.

3.4)   Snap freeze and then lyophilize the 2 mL silk nanoparticle lot in a freeze dryer overnight. After freeze-drying, reweigh the 2 mL tube and calculate the amount of silk nanoparticles (mg) that was originally present in the 2 mL sample.

3.5)   Dilute the 1 mL silk nanoparticle stock with distilled water to generate a 5-point calibration curve (0.04 – 7 mg/mL). Ensure that samples do not exceed the absorbance maximum.

3.6)   Determine the absorbance of each standard dilution at 600 nm. This is best done using a 96-well plate setup. Plot absorbance versus concentration (mg/mL) for the standard curve. Then use this standard curve routinely to determine the concentration of silk nanoparticles in suspensions.

4.   Preparation of doxorubicin-loaded silk nanoparticles

4.1)   Preparation of the doxorubicin solution

4.1.1) Dissolve 1.2 mg of doxorubicin HCl in 8 mL distilled water.

4.1.2) Make up to 10 mL with distilled water to yield a working stock of 116 μg/mL (0.2 μmol/mL).

4.2)   Preparation of doxorubicin-loaded silk nanoparticles

4.2.1) Mix 2 mL of 0.2 μmol/mL doxorubicin solution with 200 μL of 10, 30 or 50 mg/mL of silk nanoparticles in a 2 mL tube.

4.2.2) Incubate the silk-doxorubicin suspension at room temperature (25 °C) overnight on a rotating mixer.

4.2.3) Next, centrifuge the silk-doxorubicin suspension at 194,000 x g for 30 minutes. Wash the doxorubicin-loaded silk nanoparticles with distilled water and repeat this procedure twice more.

4.2.4) Pool the supernatant and note the total volume (this sample is used to determine the encapsulation efficiency).

4.2.5) Resuspend the doxorubicin-loaded silk nanoparticles in distilled water, protect from light and store at 4 ºC until use.

4.3)   Determination of encapsulation efficiency and drug loading

4.3.1) Pipet 200 μL of the supernatant from step 4.2.4 into a black microtiter plate.

4.3.2) Use a fluorescence microplate reader to measure doxorubicin-associated fluorescence at a fixed photomultiplier setting.

4.3.3) Set the excitation wavelength to 485 nm and emission wavelength to 590 nm and record the fluorescence values.

4.3.4) Generate a doxorubicin calibration curve. Ensure measurements are acquired with identical instrument settings (i.e. with a fixed photomultiplier setting). Using the calibration curve, calculate the doxorubicin concentration in the combined supernatant. Repeat this measurement in three independent experiments.

4.3.5) Use equation (1) to determine encapsulation efficiency:

(1)   Encapsulation efficiency (%) =   amount of model drug in nanoparticles x 100
                                          model drug initially added

5.   Characterization of silk nanoparticles

5.1)   Assessment of the size and zeta potential of freshly prepared and stored silk nanoparticles.

5.1.1) Store silk nanoparticles in distilled water at 4 °C and 25 °C.

5.1.2) Measure the size and zeta potential of the silk nanoparticles on days 0, 14 and 28 using dynamic light scattering (DLS). Set refractive indices to 1.33 for distilled water and 1.60 for protein [17]. Calculate particle sizes with the user interface software.

5.2)   Morphological assessment of silk nanoparticles by scanning electron microscopy (SEM).

5.2.1) Place a carbon adhesive disc onto an SEM stub and subsequently attach a silicon wafer.

5.2.2) Dilute silk nanoparticles to a concentration of 1 mg/mL. Pipette 10 µL of the sample onto a silicon wafer, freeze the sample at -80°C and lyophilize overnight using a freeze drying system as per manufacturer's instructions.

5.2.3) Coat the sample with a gold layer up to 20 nm thick using a low vacuum sputter coater.

Note: Instrument settings vary between models. The model used here is fully automated and operates by thickness only.

5.2.4) Image samples with a scanning electron microscope at 5 kV and a 40,000-fold magnification.

6.   In vitro cytotoxicity of control and doxorubicin-loaded silk nanoparticles

6.1)   Cell viability following exposure to silk nanoparticles.

6.1.1) Culture MDA-MB-231 cells in RPMI 1640 with 10%v/v FBS. Plate cells on tissue

culture treated polystyrene and incubate in a humidified 5% CO_2 atmosphere at 37 °C. Routinely subculture at 80% confluence every 2−3 days.

6.1.2) Plate MDA-MB-231 cells at a density of 2 x 10^4 cells/cm^2 in 96-well plates. Allow the cells to recover overnight.

6.1.3) Add (i) 0.001-1 μg freely diffusible doxorubicin, (ii) 0.001-0.5 mg silk nanoparticles and 0.1 mg silk nanoparticles loaded with 0.001-1 μg doxorubicin into 96-well plates (final volume 100 μL per well).

6.1.4) Determine cell viability and the half maximal inhibitory concentration (IC_{50}) by adding (3-(4,5-dimethylthiazol-2-yl)-2,5-diphenyltetrazolium bromide (MTT 5 mg/mL in PBS) at 72 hours. Incubate for 5 hours, carefully drain the wells with a pipette and dissolve the formazan with 100 μL of dimethylsulfoxide. Measure the absorbance at 560 nm. Repeat this measurement in three independent experiments.

Note: The absorbance values of untreated controls serve as a reference value for 100% cell viability.

6.2)   SEM of cells exposed to silk nanoparticles.

6.2.1) Seed MDA-MB-231 cells on sterile glass coverslips at a density of 2 x 10^4 cells/cm^2. Allow the cells to recover overnight. Expose the cells to the desired treatment conditions for 72 hours.

6.2.2) Fix the cells with 2% v/v glutaraldehyde in PBS for 30 minutes, wash with distilled water twice, dehydrate with an ethanol series, and critical point dry the samples, as detailed elsewhere[28].

6.2.3) Sputter coat the samples with a gold layer up to 20 nm thick using a low vacuum sputter coater.

Note: Instrument settings vary between models. The model used here is fully automated and operates by thickness only.

6.2.4) Image the samples by SEM using an electron acceleration of 5 kV and 700-fold magnification.

REPRESENTATIVE RESULTS:
Data were statistically analyzed as detailed previously[17]. The Student's t-test was used for sample pairs and one-way analysis of variance (ANOVA) followed by Bonferroni's multiple comparison post hoc test for multiple samples. An asterisk denotes statistical significance as follows: *P < 0.05 and **P < 0.001. All data are presented as mean values ± standard deviation (SD) and the numbers in brackets indicate the number of independent experiments.

Regenerated silk solution was prepared and subsequently added dropwise to acetone to generate silk nanoparticles via nanoprecipitation (Figure 1). This method yielded uniform (polydispersity index: 0.1), spherical, silk nanoparticles (106.5 nm ± 1.1) with a negative surface charge (-49.57 mV ± 0.6) (Figure 2 and 3). Silk nanoparticle stability in water was assessed for up to 28 days by monitoring particles size, zeta potential and morphology (Figures 2 and 3). Over the 28 day storage period, at either 4 °C or 25 °C, no significant change in particle size, charge (Figure 2) or morphology was observed (Figure 3).

Doxorubicin was used as a clinically relevant chemotherapeutic model drug for drug loading and *in vitro* cytotoxicity studies. Three different silk nanoparticle concentrations (10, 30 and 50 mg/mL) were used to assess the drug loading capacity of the silk nanoparticles. The doxorubicin encapsulation efficiency for 10, 30 and 50 mg/mL silk nanoparticles (i.e. 2, 6 or 10 mg of silk and 232 µg of doxorubicin) was 73±2.2, 87±1.8 and 97±0.2%, respectively (Figure 4A). The particle size and zeta potential of doxorubicin-loaded silk nanoparticles (10 mg) were measured and compared to 10 mg silk nanoparticle controls. The particle size did not change after drug loading (Figure 4B), while the zeta potential of doxorubicin-loaded silk nanoparticles was significantly reduced from -49.57±0.6 mV to -43.52±0.37 mV (Figure 4C).

The ability of drug-loaded silk nanoparticles to deliver doxorubicin and subsequently kill cancer cells was assessed *in vitro*. Human breast cancer MDA-MB-231 cells were exposed to silk nanoparticles, freely diffusible doxorubicin or doxorubicin-loaded silk nanoparticles. Cell viability was assessed after a 72 hours exposure period. The IC_{50} values of freely diffusible doxorubicin and doxorubicin-loaded silk nanoparticles were 0.48 µg/mL and 0.24 µg/mL, respectively while the silk nanoparticles had an IC_{50} > 5 mg/mL (Figure 5A). At equivalent drug doses of 0.1 µg, freely diffusible doxorubicin and doxorubicin-loaded silk nanoparticles caused significant decreases in cell viability of 83±11 and 65±11%, respectively (Figure 5B). However, freely diffusible doxorubicin showed a substantial greater cytotoxicity than doxorubicin-loaded silk nanoparticles. These quantitative measurements were corroborated by qualitative SEM imaging (Figure 5c). Here, control cultures showed high cellular density and a predominating mesenchymal MDA-MB-231 phenotype; similar observations were made for cultures exposed to silk nanoparticles. However, cultures exposed to doxorubicin showed a markedly different cell phenotype. At the equivalent doxorubicin dose, MDA-MB-231 cells treated with freely diffusible doxorubicin and doxorubicin-loaded silk nanoparticles showed a substantial reduction in cell numbers. Furthermore, many cells had a very broad and spread out morphology. Cultures exposed to doxorubicin-loaded silk nanoparticles showed evidence of nanoparticles (and their aggregates) associated with the plasma membrane (Figure 5C).

Figure 1: The key steps to generate a reverse engineered silk solution and silk nanoparticles. First, silk cocoons are reverse engineered by cutting and then degumming them for 60 minutes (i.e. boiling) to yield degummed silk fibers. The fibers are dissolved in 9.3 M LiBr and then dialyzed against water for 72 hours. An aqueous 5%w/v silk solution is used to generate silk nanoparticles. The dropwise addition of silk into acetone leads to silk nanoprecipitation. Silk nanoparticles are washed and collect for subsequent use.

Figure 2: Size and charge characterization of silk nanoparticles. Particle size and zeta potential of silk nanoparticles at 4 °C and 25 °C over 28 days. ±SD; error bars are hidden within the plot symbol when not visible, n = 3.

Figure 3: Quality assessment of silk nanoparticles stored at 4 °C and 25 °C over 28 days. Silk nanoparticles were imaged using scanning electron microscopy (scale bar = 1 μm).

Figure 4: Characterization of doxorubicin-loaded silk nanoparticles (Dox-SNPs). (A) Encapsulation efficiency of 232 μg doxorubicin in response to different amounts of silk nanoparticles (SNPs); 2, 6 and 10 mg of silk nanoparticles. The encapsulation efficiency for 10 mg and 5 mg silk nanoparticles significantly increased when compared to 2 mg silk nanoparticles. (B) Particle size and (C) zeta potential of doxorubicin-loaded silk nanoparticles compared to control silk nanoparticles (10 mg of silk nanoparticles). Statistically significant differences for sample pairs were determined with Student's t-test. Multiple samples were assessed by one-way ANOVA, followed by Bonferroni's multiple comparison post hoc test; *P < 0.05, **P < 0.001, ±SD; error bars are hidden within the plot-symbol when not visible, n = 3.

Figure 5: *In vitro* cytotoxicity of silk nanoparticles and doxorubicin-loaded silk nanoparticles in human breast cancer cells. (A) Cell viability of MDA-MB-231 cells after a 72 hours treatment cycle with silk nanoparticles (SNPs) (0.01-5 mg/mL); volumes per well were 100 μl. (B) Cell viability of MDA-MB-231 cells after a 72 hours treatment cycle with 0.1 mg silk nanoparticles, 0.1 μg of freely diffusible doxorubicin (Dox) or 0.1 mg of silk nanoparticles loaded with 0.1 μg of doxorubicin (Dox-SNPs). Cell viability was statistically decreased following the exposure to 0.1 μg of freely diffusible doxorubicin and 0.1 mg of silk nanoparticles loaded with 0.1 μg of doxorubicin when compared to the control. (C) SEM images of MDA-MB-231 cells exposed to (i) medium (control), (ii) 0.1 mg silk nanoparticles, (iii) 0.1 μg of freely diffusible doxorubicin, and (iv) doxorubicin-loaded silk nanoparticles at equivalent doses (scale bar = 50 μm). Statistical analysis was performed by one-way ANOVA followed by Bonferroni's multiple comparison post hoc test, ns = not significant, *P < 0.05, **P < 0.001, ±SD; error bars are hidden within the plot-symbol when not visible, n = 3.

DISCUSSION:
Various methods are available to produce silk nanoparticles, including polyvinyl alcohol blending[20], spray drying[21], salting out[22], capillary microdot printing[23], supercritical CO_2 precipitation[24] and nanoprecipitation[16,25] (reviewed in [26]) However, nanoprecipitation, due to its overall simplicity, is the most popular technique for generating silk nanoparticles. Therefore, the purpose of this study was to apply nanoprecipitation to reverse-engineered silk to manufacture silk-based nanoparticles that can be used for a range of applications, including lysosomotropic anticancer drug delivery.

Over the past decade, nanoprecipitation has become one of the most common procedures for the manufacture of protein-based nanoparticles[29]. Our research group[16,17] and others[25,26,30,31] have successfully applied this technology to silk; here, we present a simple but robust stepwise protocol for the generation of silk nanoparticles. Acetone nanoprecipitation yields spherical silk particles that are homogeneous in size and fall typically in the nanometer size range. Acetone has emerged as the preferred continuous phase over solvents such as methanol, ethanol, isopropanol

and butanol[16,25]. Acetone yields nanoparticles that have a reduced level of hydration when compared to the metastable 100–200 nm sized spherical micellar structures present in native and regenerated silk solutions[32]. However, there is scope to explore solvent mixtures and variations in degumming time in order to generate silk (nano)particles with potentially different properties to those described here. The protocol described here utilizes acetone as the continuous phase, which permits the manufacture of uniform spherical nano-sized silk particles (106.5±1.1 nm) that carry a negative surface charge (-49.57±0.6 mV) and that have a tight packing of the hydrophobic, crystalline silk chains[16,17]. Overall, the described procedure requires little hands-on time and yields silk nanoparticles from a reverse-engineered aqueous silk solution (Figure 1). Some of the key features of this procedure include the use of 60 minutes degummed silk, the appropriate drop size (approximately 10 µl/drop) and a maximum dropping rate of 50 drops/minute. Adherence to these key features results in a typical yield of 14%. These nanoparticles are robust and we provide evidence that they are stable and do not change their physical characteristics over a 28-day storage period. However, a potential caveat of the described method is the absence to generate particles over a broad size range (i.e. generating particles from the nanometer to micrometer scale while maintaining a narrow polydispersity index).

Controlling particle size, charge and shape is important for drug delivery, particularly when targeting solid tumors[33]. Particles in the 100 nm size range are emerging as ideal candidates for tumor targeting. Therefore, 100 nm sized silk nanoparticles are potential contenders as anticancer drug delivery systems for solid tumor treatments. Silk nanoparticles have a negative surface charge, which renders them easily loaded with positively charged drugs through exploitation of the electrostatic interaction[16]. However, besides charge, additional drug characteristics (e.g. logD) are also known to affect drug loading and release[34]. In the present study, doxorubicin, a weakly basic anticancer drug, was selected as a model drug candidate. The drug loading study (Figure 4) showed that increasing the silk nanoparticle concentration led to increased doxorubicin encapsulation efficiency; 10 mg of silk nanoparticles can encapsulate 232 µg of doxorubicin. Drug loading of the silk nanoparticles, in turn, resulted in silk nanoparticles with a significantly reduced surface charge, which was direct experimental evidence confirming that the doxorubicin-silk charge interaction is important for this particular drug carrier combination.

We have previously provided evidence that silk nanoparticles can serve as a lysosomotropic drug delivery system[16,17]. Here, we show a test using doxorubicin-loaded silk nanoparticles to treat the human breast cancer MDA-MB-231 cell line. These cells are derived from a highly invasive triple negative breast cancer (ER[-]/PR[-]/HER2^{-}) that is difficult to treat in the clinic[35]. Therefore, designing a drug delivery system tailored to this patient population is expected to yield tremendous benefits. In the absence of drug loading, silk nanoparticles did not affect cell viability (IC_{50} values > 5 mg/mL) (Figure 5a, c). However, at equivalent doses, significantly greater cytotoxicity was observed with freely diffusible doxorubicin than with doxorubicin-loaded silk nanoparticles (Figure 5b). The differences between the *in vitro* cellular pharmacokinetics of freely diffusible and particle bound drug explain this observation. The freely diffusible drug can rapidly cross the plasma membrane via diffusion, whereas uptake of the drug-loaded nanoparticles relies on endocytosis. Nonetheless, endocytic uptake of nanoparticles can enhance drug retention and overcome drug resistance mechanisms[3]. However, the true benefit of nanoparticle-mediated anticancer drug delivery is that it exploits the EPR

effect to facilitate passive tumor targeting and to improve pharmacokinetics. Therefore, the use of a nanoparticle-based drug delivery approach can only be fully assessed *in vivo. In vitro* studies have limitations (i.e. the absence of the EPR effect) that preclude the full characterization of these types of drug delivery systems[7].

In summary, the described methodology allows the easy manufacture of spherical silk nanoparticles of consistent size and surface charge. These silk nanoparticles can be used for a broad range of applications (e.g., cosmetics, templates for nano patterning, theranostics, lubricants, control particles for nanotoxicity studies), including their use as anticancer drug delivery platforms.

DISCLOSURES:
The authors have nothing to disclose.

REFERENCES:
1.   Haley, B. & Frenkel, E. Nanoparticles for drug delivery in cancer treatment. *Urol. Oncol.* **26** (1), 57–64, doi:10.1016/j.urolonc.2007.03.015 (2008).
2.   Sun, T., Zhang, Y. S., Pang, B., Hyun, D. C., Yang, M. & Xia, Y. Engineered nanoparticles for drug delivery in cancer therapy. *Angew. Chem. Int. Ed.* **53** (46), 12320–12364, doi:10.1002/anie.201403036 (2014).
3.   Davis, M. E., Chen, Z. G. & Shin, D. M. Nanoparticle therapeutics: an emerging treatment modality for cancer. *Nat. Rev. Drug Discov.* **7** (9), 771–782, doi:10.1038/nrd2614 (2008).
4.   Sheridan, C. Proof of concept for next-generation nanoparticle drugs in humans. *Nature Biotechnol.* **30** (6), 471–473, doi:10.1038/nbt0612-471 (2012).
5.   Matsumura, Y. & Hitoshi, M. A New Concept for Macromolecular Therapeutics in Cancer Chemotherapy: Mechanism of Tumoritropic Accumulation of Proteins and the Antitumor Agent Smancs. *Cancer Res.* **46**, 6387 (1986).
6.   De Duve, C., De Barsy, T., Poole, B., Trouet, A., Tulkens, P. & Van Hoof, F. Lysosomotropic agents. *Biochem. Pharmacol.* **23** (18), 2495–2531, doi:10.1016/0006-2952(74)90174-9 (1974).
7.   Duncan, R. & Richardson, S. C. W. Endocytosis and intracellular trafficking as gateways for nanomedicine delivery: opportunities and challenges. *Mol. Pharm.* **9** (9), 2380–402, doi:10.1021/mp300293n (2012).
8.   Vishakha, K., Kishor, B. & Sudha, R. Natural Polymers – A Comprehensive Review. *Int. J. Pharm. Biomed. Res.* **3** (4), 1597–1613 (2012).
9.   Pritchard, E. M. & Kaplan, D.L. Silk fibroin biomaterials for controlled release drug delivery. *Expert. Opin. Drug Del.* **8** (6), 797-811, doi: 10.1517/17425247.2011.568936 (2011).
10.   Thurber, A. E., Omenetto, F. G. & Kaplan, D. L. In vivo bioresponses to silk proteins. *Biomaterials.* **71**, 145–157, doi:10.1016/j.biomaterials.2015.08.039 (2015).
11.   Pritchard, E. M., Dennis, P. B., Omenetto, F., Naik, R. R. & Kaplan, D. L. Physical and chemical aspects of stabilization of compounds in silk. *Biopolymers.* **97** (6), 479–498,

doi:10.1002/bip.22026 (2012).

12.   Seib, F. P., Pritchard, E. M. & Kaplan, D. L. Self-Assembling Doxorubicin Silk Hydrogels for the Focal Treatment of Primary Breast Cancer. *Adv. Funct. Mater.* **23** (1), 58–65, doi:10.1002/adfm.201201238 (2013).

13.   Seib, F. P. & Kaplan, D. L. Doxorubicin-loaded silk films: drug-silk interactions and in vivo performance in human orthotopic breast cancer. *Biomaterials.* **33** (33), 8442–50, doi:10.1016/j.biomaterials.2012.08.004 (2012).

14.   Seib, F. P., Coburn, J., *et al.* Focal therapy of neuroblastoma using silk films to deliver kinase and chemotherapeutic agents in vivo. *Acta. Biomater.* **20**, 32–38, doi:10.1016/j.actbio.2015.04.003 (2015).

15.   Coburn, J. M., Na, E. & Kaplan, D. L. Modulation of vincristine and doxorubicin binding and release from silk films. *J. Control. Release.* **220**, 229–238, doi:10.1016/j.jconrel.2015.10.035 (2015).

16.   Seib, F. P., Jones, G. T., Rnjak-Kovacina, J., Lin, Y. & Kaplan, D. L. pH-dependent anticancer drug release from silk nanoparticles. *Adv. Healthc. Mater.* **2** (12), 1606–11, doi:10.1002/adhm.201300034 (2013).

17.   Wongpinyochit, T., Uhlmann, P., Urquhart, A. J. & Seib, F. P. PEGylated Silk Nanoparticles for Anticancer Drug Delivery. *Biomacromolecules.* **16** (11), 3712–3722, doi:10.1021/acs.biomac.5b01003 (2015).

18.   Seib, F. P. & Kaplan, D. L. Silk for Drug Delivery Applications: Opportunities and Challenges. *Isr. J. Chem.* **53** (9-10), 1-12, doi:10.1002/ijch.201300083 (2013).

19.   Yucel, T., Lovett, M. L. & Kaplan, D. L. Silk-based biomaterials for sustained drug delivery. *J. Control. Release.* **190**, 381–397, doi:10.1016/j.jconrel.2014.05.059 (2014).

20.   Wang, X., Yucel, T., Lu, Q., Hu, X. & Kaplan, D. L. Silk nanospheres and microspheres from silk/pva blend films for drug delivery. *Biomaterials.* **31** (6), 1025–35, doi:10.1016/j.biomaterials.2009.11.002 (2010).

21.   Qu, J., Wang, L., Hu, Y., You, R. & Li, M. Preparation of Silk Fibroin Microspheres and Its Cytocompatibility. *J. Biomater. Nanobiotechnol.* **4**, 84–90, doi:10.4236/jbnb.2013.41011 (2013).

22.   Lammel, A., Hu, X., Park, S., Kaplan, D. & Scheibel, T. Controlling silk fibroin particle features for drug delivery. *Biomaterials.* **31** (16), 4583–4591, doi:10.1016/j.biomaterials.2010.02.024. (2010).

23.   Gupta, V., Aseh, A., Ríos, C. N., Aggarwal, B. B. & Mathur, A. B. Fabrication and characterization of silk fibroin-derived curcumin nanoparticles for cancer therapy. *Int. J. Nanomedicine.* **4**, 115–22 (2009).

24.   Zhao, Z., *et al.* Generation of silk fibroin nanoparticles via solution-enhanced dispersion by supercritical CO_2. *Ind. Eng. Chem. Res.* **52** (10), 3752–3761, doi:10.1021/ie301907f (2013).

25.   Tudora, M., Zaharia, C. & Stancu, I. Natural silk Fibroin micro-and nanoparticles with potential uses in drug delivery systems. *U.P.B. Sci. Bull., Series B.* **75** (1), 43–52 (2013).

26.   Zhao, Z., Li, Y. & Xie, M.-B. Silk Fibroin-Based Nanoparticles for Drug Delivery. *Int. J. Mol. Sci.* **16** (3), 4880–4903, doi:10.3390/ijms16034880 (2015).

27.   Rockwood, D., Preda, R. & Yücel, T. Materials fabrication from Bombyx mori silk fibroin. *Nat. Protoc.* **6** (10), 1–43, doi:10.1038/nprot.2011.379 (2011).

28.   Seib, F. P., Müller, K., Franke, M., Grimmer, M., Bornhäuser, M. & Werner, C. Engineered extracellular matrices modulate the expression profile and feeder properties of bone marrow-derived human multipotent mesenchymal stromal cells. *Tissue. Eng. Part A.* **15** (10),

3161–3171, doi:10.1089/ten.tea.2008.0600 (2009).

29.   Lai, P., Daear, W., Löbenberg, R. & Prenner, E. J. Overview of the preparation of organic polymeric nanoparticles for drug delivery based on gelatine, chitosan, poly(d,l-lactide-co-glycolic acid) and polyalkylcyanoacrylate. *Colloids Surf., B, Biointerfaces.* **118**, 154–63, doi:10.1016/j.colsurfb.2014.03.017 (2014).

30.   Subia, B. & Kundu, S. C. Drug loading and release on tumor cells using silk fibroin-albumin nanoparticles as carriers. *Nanotechnology.* **24** (3), 035103, doi:10.1088/0957-4484/24/3/035103 (2013).

31.   Zhang, Y. Q., Shen, W. D., Xiang, R. L., Zhuge, L. J., Gao, W. J. & Wang, W. B. Formation of silk fibroin nanoparticles in water-miscible organic solvent and their characterization. *J. Nanopart. Res.* **9** (5), 885–900, doi:10.1007/s11051-006-9162-x (2006).
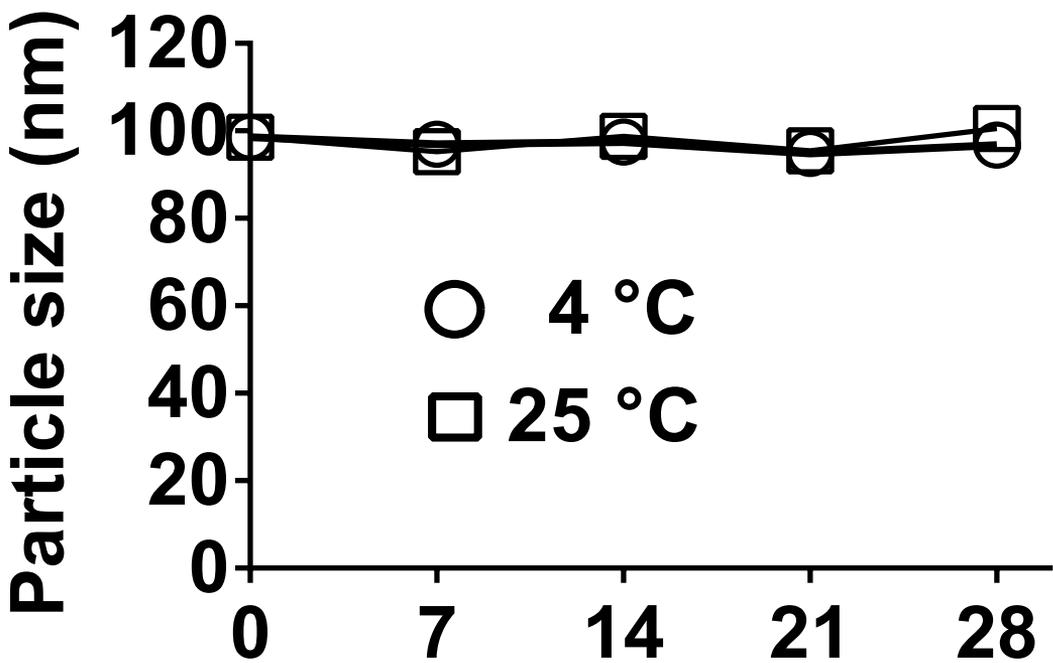
32.   Jin, hr. J. & Kaplan, D. L. Mechanism of silk processing in insects and spiders. *Nature.* **424** (6952), 1057–1061, doi:10.1038/nature01809 (2003).

33.   Bae, Y. hr. & Park, K. Targeted drug delivery to tumors: myths, reality and possibility. *J. Control. Release.* **153** (3), 198–205, doi:10.1016/j.jconrel.2011.06.001 (2011).

34.   Lammel, A., Schwab, M., Hofer, M., Winter, G. & Scheibel, T. Recombinant spider silk particles as drug delivery vehicles. *Biomaterials.* **32** (8), 2233–40, doi:10.1016/j.biomaterials.2010.11.060 (2011).

35.   Holliday, D. L. & Speirs, V. Choosing the right cell line for breast cancer research. *Breast. Cancer. Res.* **13**, 215, doi:10.1186/bcr2889 (2011).
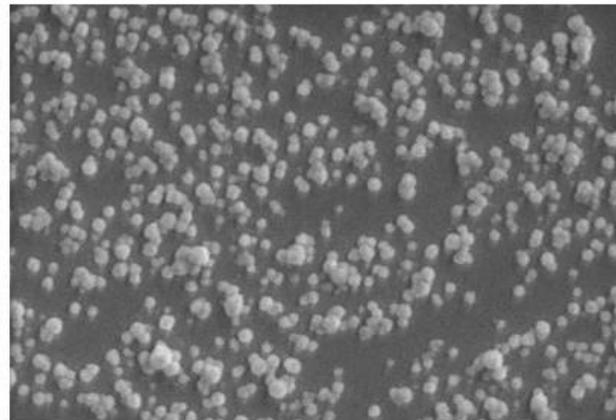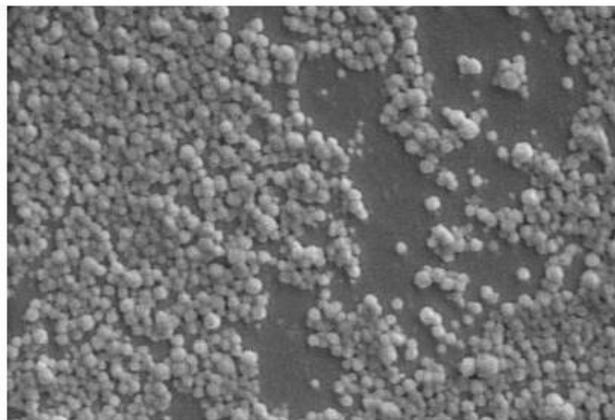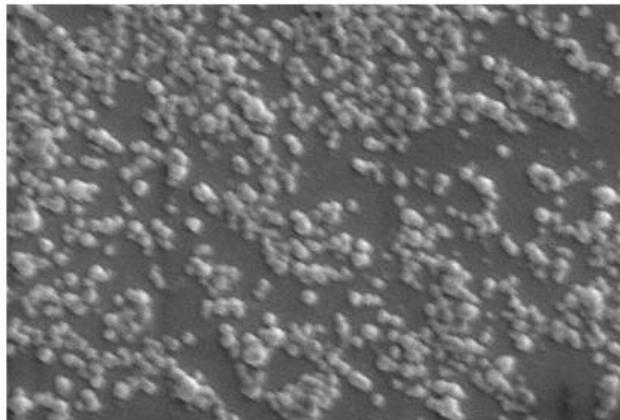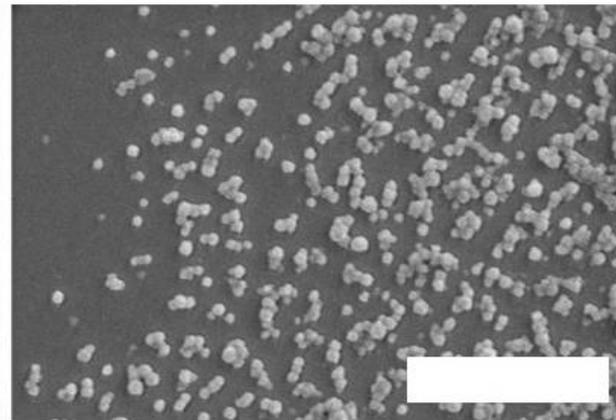
B. mori cocoons 9 cm → 30 min → **Cut cocoons** 7 cm → 60 min → **Degumming process** → 12 h → **Degummed silk** 9 cm

↓ 4 h

Degummed silk dissolved in LiBr ← 15 min ← **Dialysis against water** ← 72 h ← **Silk solution (5 wt%)**

Silk solution (5 wt%) → Add dropwise to acetone 20 min → **Silk precipitation** → 2 h → **Centrifuge** → **Decant supernatant** → **Wash pellet with H₂O** → **Dispersed by sonication** → Centrifuge

Wash pellet with H₂O → 7 h → **Silk nanoparticles**

A

Cell viability (% of control) vs SNPs (mg/ml)

B

Cell viability (% of control)

| SNPs | - | + | - | + |
| Dox | - | - | + | + |

ns

**

*

C

i ii

iii iv